Meridional Localization of Planetary Waves in Stochastic Zonal Flows

ADAM HUGH MONAHAN* AND LIONEL PANDOLFO

Department of Earth and Ocean Sciences, and Crisis Points Group, Peter Wall Institute for Advanced Studies, University of British Columbia, Vancouver, British Columbia, Canada

(Manuscript received 4 June 1999, in final form 12 May 2000)

ABSTRACT

The effect of stochastic fluctuations in the zonal-mean velocity field on the energy dispersion of planetary stationary waves is considered, using the nondivergent, barotropic vorticity equation. It is found that for small noise levels, the oscillatory structure of the solutions is not altered. However, for noise levels comparable to or larger than those observed in the circulation at 500 mb, the marginal density functions of the solution process in the subpolar region cluster near zero. This indicates that fluctuations in the velocity field inhibit the poleward dispersion of stationary wave energy. This localization phenomenon appears whether the ensemble average of the mean zonal flow is superrotation or has a simple two-jet structure.

1. Introduction

Since the early work of Hoskins and Karoly (1981), a substantial amount of research has been directed toward understanding the dynamics of planetary waves in a spherical atmosphere. This subject has attracted interest because of the possible role of these global-scale waves in mediating observed atmospheric teleconnections, suggesting the possibility of a theory of large-scale, low-frequency variability in which the planetary waves play the role of fundamental dynamical elements [up-to-date reviews are given by Lau (1997) and by Trenberth et al. (1998)].

The WKB paradigm employed by Hoskins and Karoly (1981) permits calculation of approximate wavelike solutions to the nondivergent, barotropic vorticity equation linearized around a (smoothly) spatially varying background flow. Hoskins and Karoly found that disturbances with very long zonal wavelength (in particular wavenumbers 1 and 2) can propagate a great distance poleward from a subtropical source and that the amplitude of the wave generally increases poleward. The fundamental results of WKB theory for stationary waves on a zonally uniform background flow are reviewed in section 6.3 of Held (1983).

The dynamics of small perturbations, both stationary and low frequency, on a zonally inhomogeneous background flow were considered by Karoly (1983) and Branstator (1983). Karoly (1983) derived and applied the relevant WKB theory, while Branstator (1983) solved numerically the linearized, steady nondivergent barotropic vorticity equation and interpreted the results in terms of WKB theory. Branstator found that WKB theory provided a good description of the spatial structure and extent of the model's responses to steady forcing when linearization was done around either a simple background flow or a smooth climatological January 300-mb flow. Hoskins and Ambrizzi (1993) extended Branstator's result by performing time integrations of the nondivergent barotropic vorticity equation linearized around the climatological December–February (DJF) 300-mb flow. They found again that the results are in close correspondence to the predictions of WKB theory, producing in particular a zonal waveguide extending from North Africa to the East Asian Jet entrance. Li and Nathan (1994, 1997) further extended this analysis, considering the dispersion of low-frequency waves on both zonally averaged and longitudinally varying background flows. They found that, in some cases, wavelike disturbances were able to extract energy locally from the background mean flow so that a disturbance originating in the Tropics can in fact be amplified in the midlatitudes. In a series of diagnostic studies, Kiladis et al. (1992a,b, 1994, 1997) used lagged cross-correlation analysis to investigate the relations between atmospheric large-scale circulation and tropical convection. Their results reveal the presence of wave-train-like features associated with tropical convection in both the 6–30 day and 30–70 day frequency bands. They indicate

* Current affiliation: Institut für Mathematik, Humboldt-Universität zu Berlin, Berlin, Germany.

Corresponding author address: Dr. Lionel Pandolfo, Dept. of Earth and Ocean Sciences, University of British Columbia, 6270 University Boulevard, Vancouver, BC V6T 1Z4, Canada.
E-mail: lionel@ocgy.ubc.ca

that convection episodes in the eastern Indian and western Pacific Oceans force extratropical circulation anomalies, while eastern Pacific convection is forced by tropical–extratropical transients propagating into a region of upper-tropospheric westerlies. These results are broadly consistent with the linear modeling studies cited previously.

In all of the modeling studies considered above, the background wind field around which the dynamical equations were linearized was smooth: usually superrotation, a simplified two-jet structure, or boreal wintertime climatological flow. However, the *actual* flow at any given time is not nearly so smooth as is climatology, but contains a significant amount of small-scale variability. Using U.S. National Meteorological Center [NMC, now known as the National Centers for Environment Prediction (NCEP)] 300-mb twice-daily analyses, Pandolfo and Sutera (1991) showed that if the zonal wind field is considered to be a stochastic process, then the mean of the wavelike solutions to the vorticity equation linearized around these zonal wind realizations can be significantly different from the solution to the vorticity equation linearized around the time mean background flow (i.e., climatology). In particular, the poleward amplification characterizing the solution to the equation linearized around the time mean background flow was reduced in the ensemble mean of the solutions. Mathematically, this translates into the inequality:

$$\Psi \neq E\{\psi\}, \tag{1}$$

where Ψ is the solution of $\mathcal{L}(E\{U\})\Psi = S$ and $E\{\psi\}$ is the ensemble average of solutions ψ to $\mathcal{L}(U)\psi = S$. Here $\mathcal{L}(U)$ represents the differential operator associated with the steady, nondivergent barotropic vorticity equation linearized around the zonal flow U, and S is a vorticity source.

The results of Pandolfo and Sutera imply that small-scale, ''noisy'' fluctuations in the background wind field can enhance to some extent the meridional localization of perturbation energy. This result is consistent with a class of phenomena often referred to collectively as Anderson localization. First discussed in the context of condensed matter physics (Anderson 1958), it was noted that wavelike, propagating solutions to a system of equations become localized around the source (more exactly, asymptotically decaying in an exponential manner) if the effective ''refractive index'' contains random fluctuations.

Modifications to the dispersion relation of Rossby waves in a random background flow were considered by Keller and Veronis (1969) and over random topography by Thomson (1975) and Vanneste (2000a,b). They found that the presence of small-scale fluctuations introduced an imaginary part to the component of the wavenumber along the direction of the fluctuations, implying an exponential decay of the coherent wave in this direction. Since these studies considered the coherent wave, possible localization of total wave energy could not be determined. Further, the calculations in the first two of these studies were carried out using a perturbative method [described in the appendix of Keller and Veronis (1969)], which assumes that the fluctuations in bathymetry or background flow are small compared to the mean of these quantities. This approximation is too restrictive for the atmospheric problem we wish to consider, in which the fluctuations are $O(1)$.

A more general approach to the problem of wave localization due to random topography in the case of surface gravity waves has been considered by Devillard et al. (1988) and in the case of Rossby waves by Sengupta et al. (1992) for barotropic flow and by Sengupta (1994) for two-layer flow. These studies invoke a battery of results from the theory of random matrices (Kotani 1986) to calculate the decay length scale, which turns out to be the Lyapunov exponent of the solution process. This approach is a powerful tool for the calculation of localization lengths, but because it is formulated as an initial value problem on an unbounded domain, it is unclear how it would be applied to the spherical topology in which we are interested.

In this study, we use a Monte Carlo technique to extend the work of Pandolfo and Sutera (1991). The question we are addressing is: Given the joint probability density function of the stochastic process representing the background zonal-mean zonal wind field, what is the distribution of solution processes to the nondivergent, barotropic vorticity equation linearized around realizations of this background wind field? In particular, to what extent are solution processes localized around the source relative to the solution of the equations linearized around a smooth, deterministic background flow? The approach taken is to sample the distribution of solution processes by generating realizations of the background zonal-mean zonal wind and solving numerically the equations of motion linearized around this field, subject to localized forcing. We are not concerned with the ultimate origins of the forcing. In fact, Held et al. (1989) demonstrated that the linear extratropical response to tropical forcing is due primarily to the local flux convergence of transient eddies. All that is of concern in this study is that a localized source of Rossby wave energy exists.

The climatological flow around which the equations of motion have been linearized in other studies is not a state, in phase space, which is often visited by the real atmosphere (Pandolfo 1993). It is a plausible background state around which to linearize the dynamics, but excessively smooth. In this study, we will investigate the meridional structure of Rossby wave–like perturbations by linearizing about other, equally plausible, but less-smooth background zonal-mean zonal flows.

2. Statistical structure of observed winds

The dataset we consider is global 10-day lowpass-filtered 500-mb zonal velocity on a $5^\circ \times 5^\circ$ grid for the

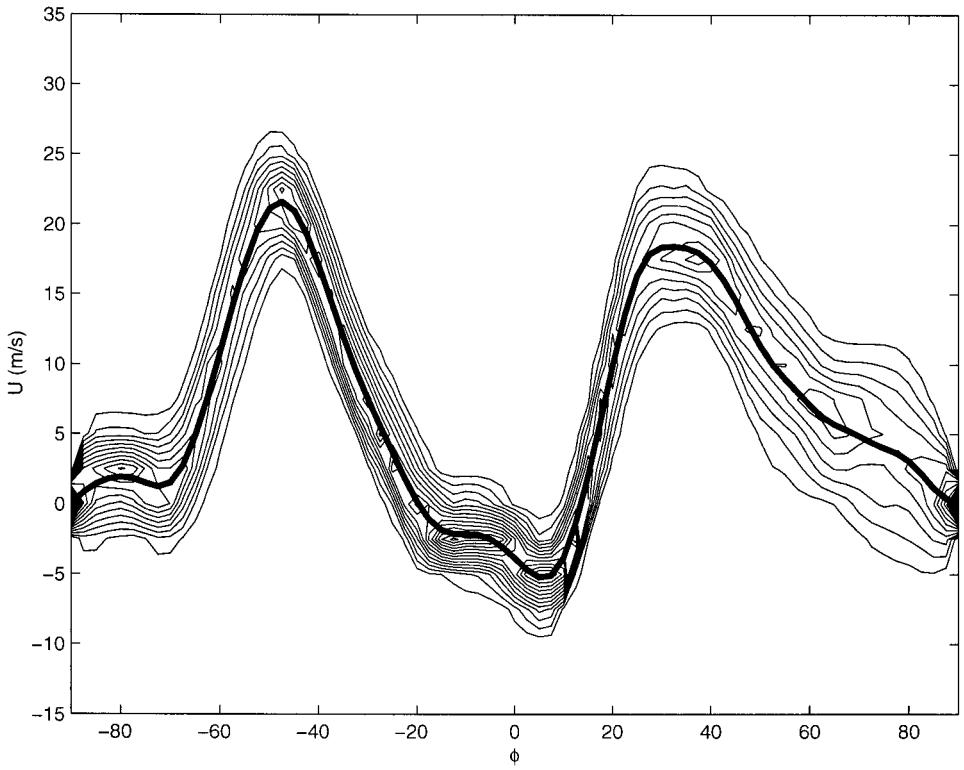

FIG. 1. Sample PDF of observed zonal-mean zonal velocity. Contour interval: 0.05.

DJF season from 1958–59 to 1997–98 from the NCEP–National Center for Atmospheric Research (NCEP–NCAR) reanalysis data (Kalnay et al. 1996). The data at each point in time are averaged around parallels of latitude to produce the zonal-mean zonal velocity fields. Figure 1 displays a contour plot of the estimated marginal probability density functions (PDFs) at each latitude for the zonal-mean zonal wind, overlayed with the sample mean (i.e., the climatological flow). The climatological flow displays the familiar midlatitude jets and weak tropical easterlies. At all latitudes, the distribution is symmetric about the mean, and its width varies only weakly with latitude, broadening somewhat toward the North Pole.

The spatial autocorrelation of the zonal-mean zonal wind (Fig. 2a) displays structure of large spatial scale. In particular, points separated by about 30° tend to be anticorrelated, corresponding in midlatitudes to the familiar index-cycle variability (Robinson 1996).

3. Spectral model

We consider the nondivergent, barotropic vorticity equation on a sphere:

$$\partial_t \nabla^2\Psi - \frac{\partial_\phi \Psi}{a}\frac{\partial_\lambda \nabla^2\Psi}{a\cos\phi} + \frac{\partial_\lambda \Psi}{a\cos\phi}\left(\frac{\partial_\phi \nabla^2\Psi}{a} + \frac{2\Omega}{a}\cos\phi\right) + \mu\nabla^2\Psi = 0, \quad (2)$$

where λ and ϕ are the zonal and meridional coordinates, respectively, Ψ is the streamfunction, a is the earth's radius, Ω is its angular frequency of rotation, and μ is an Ekman friction parameter. In spherical polar coordinates, the Laplacian is given by

$$\nabla^2\Psi = \frac{1}{a^2\cos^2\phi}[\cos\phi\partial_\phi(\cos\phi\partial_\phi\Psi) + \partial^2_{\lambda\lambda}\Psi]. \quad (3)$$

We simplify equation (2) by assuming Ψ is composed of a latitudinally varying background zonal flow plus a small perturbation with vanishing zonal average:

$$\Psi = -a\int^{\phi} d\phi' U(\phi') + \psi'(\lambda, \phi, t). \quad (4)$$

The background zonal wind $U(\phi)$ is a stochastic process. The deterministic case can be considered a limiting situation for which the distribution of $U(\phi)$ is a delta function at each latitude.

Linearizing (2) about the background wind U yields:

$$\partial_t\nabla^2\psi' + \frac{1}{a\cos\phi}U\partial_\lambda\nabla^2\psi' - \frac{1}{a\cos\phi}(\partial_\lambda\psi')\left(\partial_\phi\nabla^2\int^{\phi} d\phi' U(\phi')\right) + \frac{2\Omega}{a^2}\partial_\lambda\psi' + \mu\nabla^2\psi' = 0. \quad (5)$$

Assuming a stationary wave form for ψ':

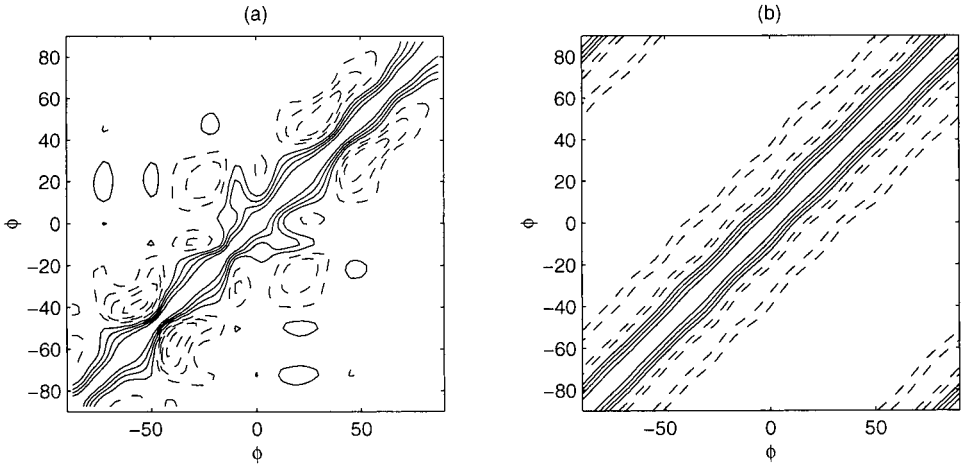

FIG. 2. Sample spatial autocorrelation of (a) observed and (b) modeled zonal-mean zonal velocity. Contour interval: 0.2. Negative contours are dashed and the zero contour is suppressed.

$$\psi'(\lambda, \phi) = \mathrm{Re}[\psi(\phi) \exp il\lambda], \tag{6}$$

and adding a source term $S(\phi)$, the nondivergent barotropic vorticity equation linearized about the background zonal flow U becomes the ODE in ϕ:

$$\left(U - \frac{i\mu a \cos\phi}{l}\right)\left[\cos\phi \frac{d}{d\phi}\left(\cos\phi \frac{d}{d\phi}\psi\right) - l^2\psi\right] - \left\{\cos^2\phi \frac{d}{d\phi}\left[\frac{1}{\cos\phi}\frac{d}{d\phi}(U\cos\phi)\right]\right\}\psi + (2\Omega a \cos^3\phi)\psi = S(\phi). \tag{7}$$

This equation is exactly equation 6.12 of Held (1993), and for $\mu = 0$ reduces to equation (A10) of Pandolfo and Sutera (1991). Under a change of variables to Mercator coordinates, it is obvious that there is always a latitude poleward of which the solutions are evanescent. As in Mercator coordinates the pole is removed to infinity, we obtain the boundary conditions:

$$\psi(-\pi/2) = \psi(\pi/2) = 0. \tag{8}$$

In Eq. (7), the stochastic processes $U(\phi)$ and $\psi(\phi)$ are multiplied together. Expressing this equation formally as

$$\mathcal{L}(U)\psi = S, \tag{9}$$

this implies that in general the mean $E\{\psi\}$ of solution processes to the equation $\mathcal{L}(U)\psi = S$ will *not* equal the solution process Ψ to the equation with the mean operator $\mathcal{L}(E\{U\})\Psi = S$. Pandolfo and Sutera (1991) pointed out that in consequence the Rossby wave solution to the equation linearized around a climatological mean zonal flow need not bear any resemblance to the average of wave solutions to the equations linearized around individual realizations of the background flow. The stochastic boundary value problem (7) thus possesses a richness not present in previous deterministic studies.

Because U is in general not smooth, we cannot use WKB theory to solve (7), and instead turn to numerical methods. Equation (7) is naturally discretized by recasting it in spectral form. The natural Fourier basis on the domain $[-\pi/2, \pi/2]$ is the orthogonal set of functions $\exp 2in\phi$, $n = -\infty, \ldots, \infty$. The function $\psi(\phi)$ is expanded on this basis as

$$\psi(\phi) = \sum_{m=-\infty}^{\infty} \psi_m e^{2im\phi}, \tag{10}$$

where the expansion coefficients ψ_m are given by

$$\psi_m = \frac{1}{\pi}\int_{-\pi/2}^{\pi/2} d\phi \psi(\phi) e^{-2im\phi}. \tag{11}$$

Similar expansions hold for U and S. Substituting these expansions into Eq. (7), we obtain the infinite set of coupled algebraic equations for the ψ_m:

$$\sum_{m=-\infty}^{\infty} M_{nm}\psi_m = S_n, \tag{12}$$

where

$$M_{nm} = \left(n - \frac{1}{2}\right)(n - 2m - 1)U_{n-m-1} + [2(n-m)^2 + 1 - 2m^2 - l^2]U_{n-m} + \left(n + \frac{1}{2}\right)(n - 2m + 1)U_{n-m+1} + 2\Omega a C_{n-m} + \frac{i\mu a}{l}\left[m\left(m + \frac{1}{2}\right)D_{n-m-1} + (2m^2 + l^2)D_{n-m} + m\left(m - \frac{1}{2}\right)D_{n-m+1}\right]. \tag{13}$$

The coefficients

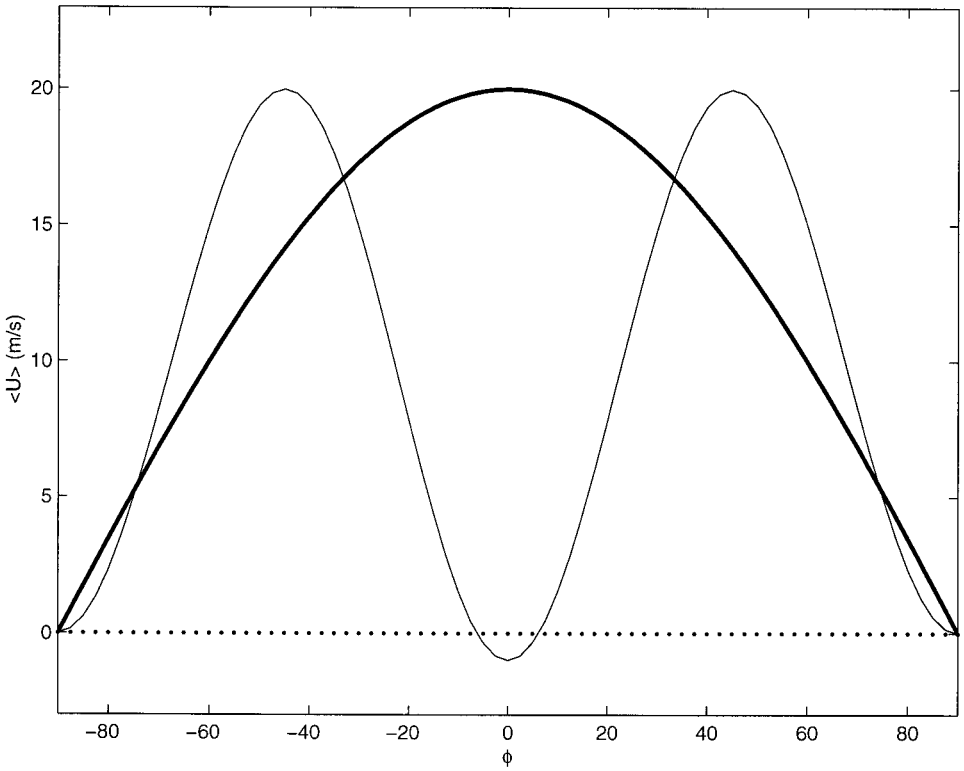

FIG. 3. Mean background flow profiles, for superrotation flow (thick line), and simple two-jet flow (thin line). The dotted line is at $\langle U \rangle = 0$.

$$C_m = \frac{12}{\pi}(-1)^m \frac{1}{(1 - 4m^2)(9 - 4m^2)} \tag{14}$$

are the Fourier components of $\cos^3\phi$, and

$$D_m = \frac{2}{\pi}(-1)^m \frac{1}{1 - 4m^2} \tag{15}$$

are the Fourier components of $\cos\phi$.

For numerical implementation, Eq. (12) must be truncated to a finite number $2N + 1$ of Fourier components, yielding the approximate equation

$$\sum_{m=-N}^{N} M_{nm}\psi_m = S_n. \tag{16}$$

Throughout this study, we used a value of $N = 50$. Sensitivity studies indicate that increasing the number of modes N does not change the results. It is worthwhile to note that the truncated spectral model we have adopted is superior to, say, a finite-difference approximation, because the latter involves errors both due to limited resolution and finite differencing of derivatives. In a spectral model all derivatives are performed exactly, and the only error is associated with truncation of the Fourier series.

We model the zonal wind by the equation

$$U(\phi) = \tilde{U}(\phi) + \eta U_{\max} R(\phi), \tag{17}$$

where $\tilde{U}(\phi)$ represents the resulting mean background wind profile, η tunes the standard deviation of the fluctuations, $U_{\max}$ is the maximum value of $\tilde{U}(\phi)$, and $R(\phi)$ is a stationary, mean-zero, unit-variance stochastic process with an oscillating and exponentially decaying autocovariance function:

$$E\{R(\phi)\} = 0, \tag{18}$$

$$E\{R^2(\phi)\} = 1, \tag{19}$$

$$E\{R(\phi)R(\phi + \phi_0)\} = \exp(-\phi_0^2/2r^2)\cos(2a\phi_0), \tag{20}$$

with $\tau = 25°$ and $\alpha = 3$. These parameter values were selected so that the spatial autocorrelation function of the simulated U process (Fig. 2b) matched reasonably well that of the observed winds (Fig. 2a). The correlation of the wind field at the antipodes is an artifact arising because realizations of the $R(\phi)$ process were generated on a spectral domain, as described in the appendix.

Because this study is primarily interested in the variability of forced wave structures arising from fluctuations in the mean flow, we are not particularly concerned with the details of how the waves are forced. Thus, throughout the study, we employ a simple, narrow Gaussian forcing of unit amplitude:

$$S(\phi) = \frac{1}{\sqrt{2\pi\sigma}} \exp[-(\phi - \phi_F)^2/2\sigma^2], \tag{21}$$

where $\sigma = 1°$.

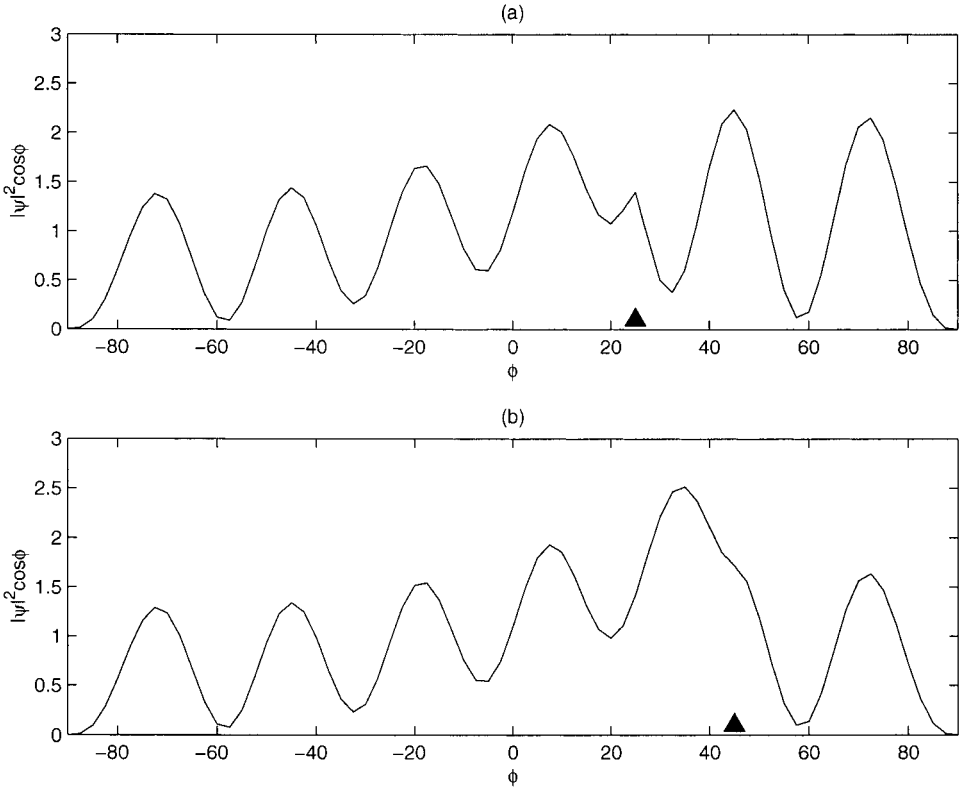

FIG. 4. Normalized $|\psi|^2 \cos\phi$ for superrotation flow, with forcing at (a) 25°N, (b) 45°N. The source location is illustrated by the black triangle.

4. Superrotation flow

The first set of experiments considered a background zonal-mean wind of constant angular velocity, a so-called superrotation flow:

$$\tilde{U}(\phi) = U_{\max} \cos\phi. \tag{22}$$

Because it is of such a simple structure, the propagation of Rossby-type waves in such a background flow field (shown in Fig. 3) has been considered several times in the literature (e.g., Hoskins and Karoly 1981; Branstator 1983; Yang and Hoskins 1996). The associated relative vorticity field has the same latitudinal structure as the planetary vorticity, so the superrotation flow affects the propagation of Rossby waves by either amplifying or attenuating the background potential vorticity gradient:

$$\partial_\phi(\zeta + f) = 2\left(\frac{U_{\max}}{a} + \Omega\right)\cos\phi. \tag{23}$$

For westerly superrotation flow, the potential vorticity gradient is augmented, and wavelike disturbances experience a stronger meridional restoring force (Pedlosky 1987).

We consider a series of experiments using superrotation flow with $U_{\max} = 20$ m s^{-1} and with weak friction, $\mu = (30 \text{ days})^{-1}$. Figure 4 plots $\psi^2 \cos\phi$ for the $l = 1$ wave, normalized to unity, for forcing at $\phi_F = 25°$N and $\phi_F = 45°$N in the limit of zero noise, $\eta = 0$. The product $\psi^2 \cos\phi$ is a measure of the energy per unit area in the perturbation. Note that on either side of the forcing, the amplitude of the oscillatory function $\psi^2 \cos\phi$ decays slowly away from the source. In the limit of zero friction, $\mu \to 0$, the amplitude is constant (not shown). This is precisely the result predicted by Hoskins and Karoly (1981) using WKB theory. Their approximate result for superrotation flows with $\mu = 0$ yielded oscillatory solutions for which

$$\psi \sim \cos^{-1/2}\phi. \tag{24}$$

For the case of a smooth superrotation background flow, then, the $l = 1$ wave is global in meridional extent, and the energy per unit area diminishes poleward only weakly.

We now consider the effect of fluctuations in the background wind. For $\eta \neq 0$, the distribution of $|\psi|^2 \cos\phi$ at any latitude is no longer a delta function. Figure 5 displays plots of the marginal distribution $P(|\psi|^2 \cos\phi)$ and the sample mean $\langle \psi^2 \cos\phi \rangle$ for values of η in increments of 0.05 from 0.05 to 0.4. These were estimated from 1000 realizations of $U(\phi)$ at each noise level. For each realization, $|\psi|^2 \cos\phi$ has been normalized to unity, because we are more concerned with the meridional structure of the response than its overall amplitude. At

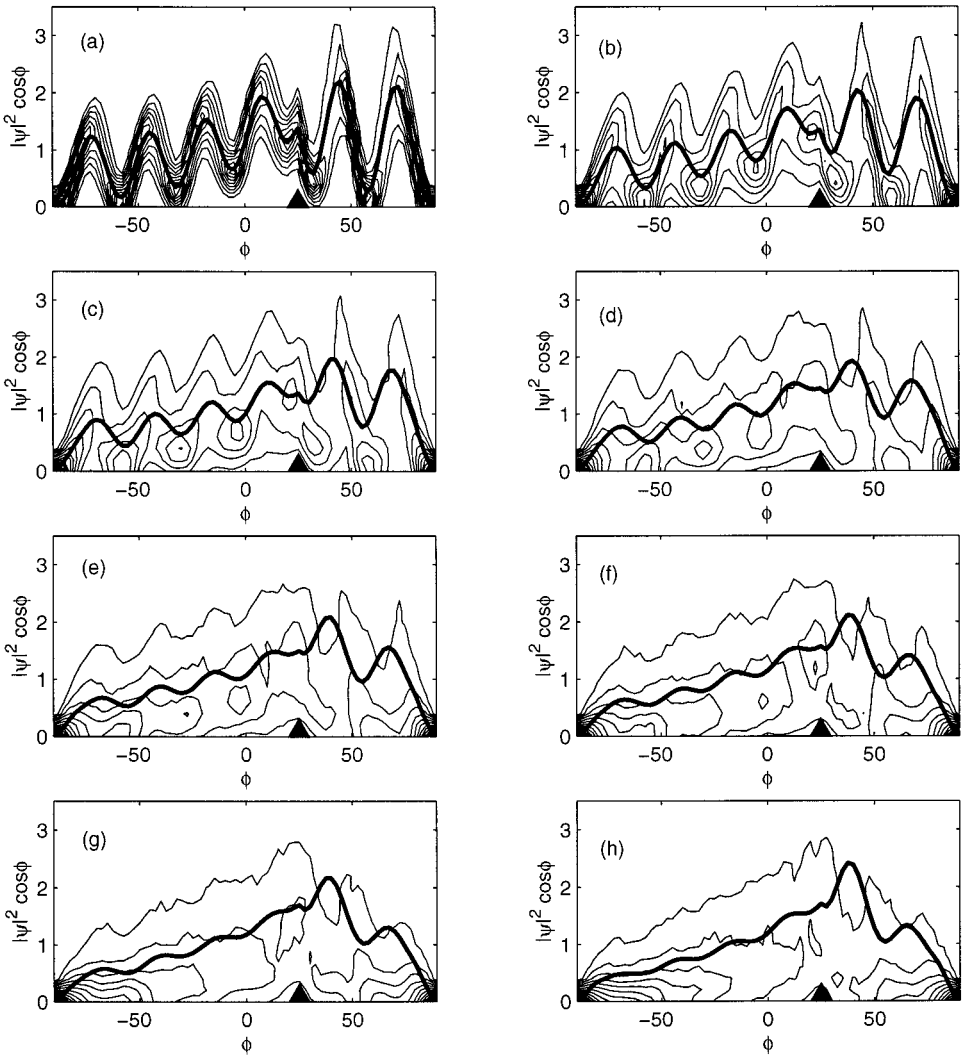

FIG. 5. Estimated PDF of $|\psi|^2 \cos\phi$ as a function of latitude for superrotation flow, for noise levels in increments of 0.05 from (a) $\eta = 0.05$ to (h) $\eta = 0.4$. The bold line is the sample mean $\langle|\psi|^2 \cos\phi\rangle$. The source location, $\phi_F = 25°$N, is marked by the black triangle. Contour interval: 0.04.

$\eta = 0.05$, the distribution of $|\psi(\phi)|^2 \cos\phi$ broadens about the noise-free solution, but retains an essentially oscillatory character. This is reflected in the structure of the mean $\langle|\psi|^2 \cos\phi\rangle$. As η is increased, the poleward attenuation of $\langle|\psi|^2 \cos\phi\rangle$ increases and the strength of the oscillations reduces. Furthermore, the PDF of $|\psi|^2 \cos\phi$ begins to concentrate near zero, especially near the poles, although the PDF retains the hint of an oscillatory structure. This concentration of the PDF near zero becomes especially marked as η is increased through $\eta \simeq 0.2$, beyond which point the marginal PDF no longer retains any manifest oscillatory character. For these noise levels, the concentration of the PDF near zero in the high latitudes (and into the midlatitudes as η increases) indicates that it is increasingly common that solutions are trapped around the source, with no appreciable dispersion of energy to the vicinity of the poles. The excluded region grows with the strength of the fluctuations in the background wind. The fluctuations in U have thus resulted in a *localization* of the stationary wave energy.

The effect of fluctuations in U on the response to a source at 45°N is displayed in Fig. 6. As was the case with the source at 25°N, for small noise level η the oscillatory character of the PDF and mean of $|\psi|^2 \cos\phi$ is unchanged. As η increases, the PDF and sample mean lose their oscillatory character even more rapidly than was the case with the source location at $\phi_F = 25°$N. Marked localization appears to set in for noise levels slightly higher than $\eta = 0.15$.

Thus, fluctuations in the background zonal wind reduce the poleward dispersion of stationary wave energy. This effect increases as the strength of the fluctuations increases.

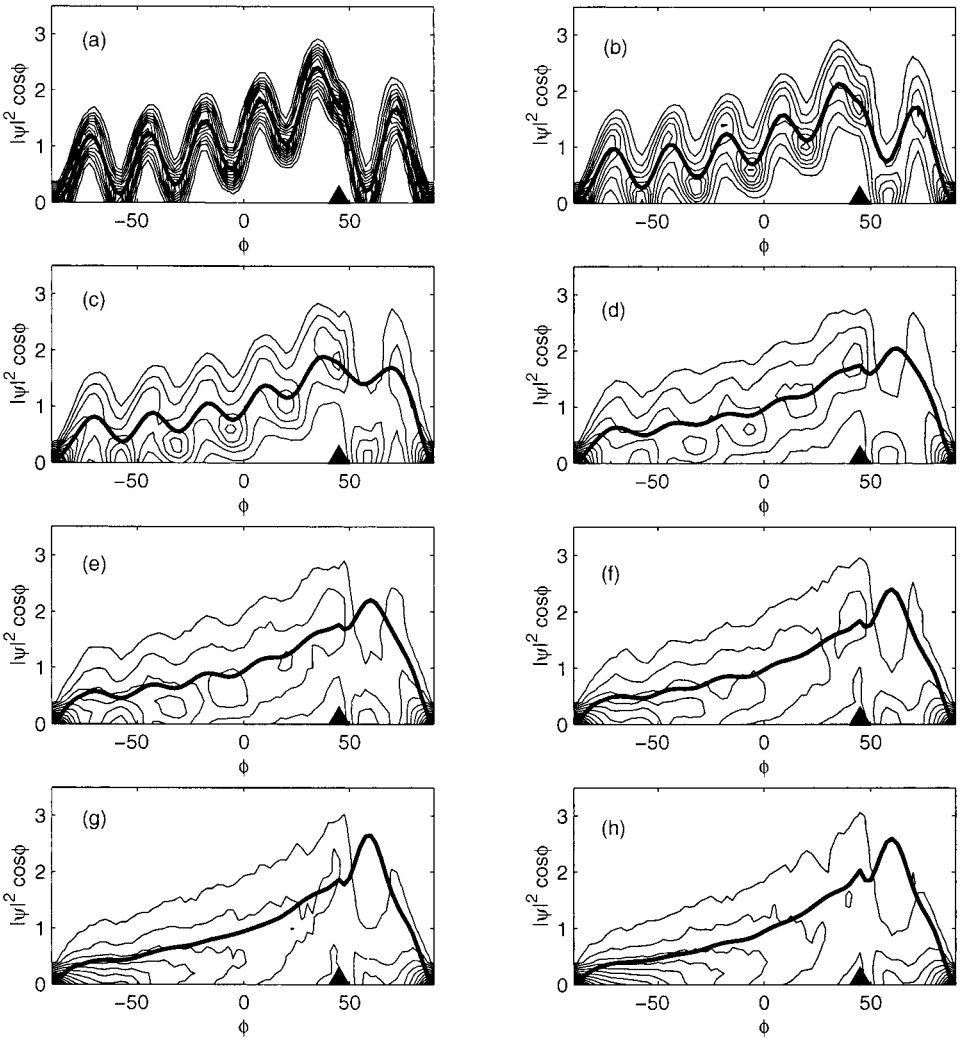

FIG. 6. As in Fig. 5 with the source located at $\phi_F = 45°$N.

5. Two-jet flow

A second set of experiments was carried out for which the zonal-mean background flow assumed the simple two-jet structure:

$$\tilde{U}(\phi) = U_{\text{jet}}[\sin^2 2\phi - a \exp(-\phi^2/2b^2)], \qquad (25)$$

with parameter values $U_{\text{jet}} = 20$ m s^{-1}, $a = -0.05$, and $b = 16°$ chosen so that $\tilde{U}(\phi)$, shown in Fig. 3, resembles the observed climatological zonal-mean zonal wind at 500 mb (Fig. 1), with strong westerly midlatitude jets and weak tropical easterlies. Figure 7 displays normalized $|\psi|^2 \cos\phi$ for forcing at $\phi_F = 10°$N, with $\eta = 0$. Comparing this result to those obtained for superrotation flow (Fig. 4), we see confinement of perturbation energy to the hemisphere in which the source is located. This is consistent with absorption, reflection, or overreflection of wave energy at a critical line, which, for stationary Rossby waves, is $U = 0$. The inhibition of meridional dispersion due to the presence of critical lines is a generic feature of linearized models (Held 1983). This is discussed further in the next section.

Again, we consider the dispersion characteristics of the perturbation response to forcing localized at 10°N for randomly fluctuating background flows, where now the ensemble mean background wind is given by (25). Marginal distributions and sample means of $|\psi|^2 \cos\phi$ are shown in Fig. 8 for η in increments of 0.05 from 0.05 to 0.4. For low noise levels, the marginal distributions broaden around the delta-function distribution associated with $\eta = 0$, as was the case when the mean background flow was a superrotation, and the collection of distributions retains an essentially oscillatory character. Note that the introduction of fluctuations in the background flow allows some interhemispheric dispersion of wave energy. As η increases, the amplitude of the peak of $\langle |\psi|^2 \cos\phi \rangle$ near the source grows while those of the peaks away from the source diminish. As was the case with the superrotation flow, the PDFs of

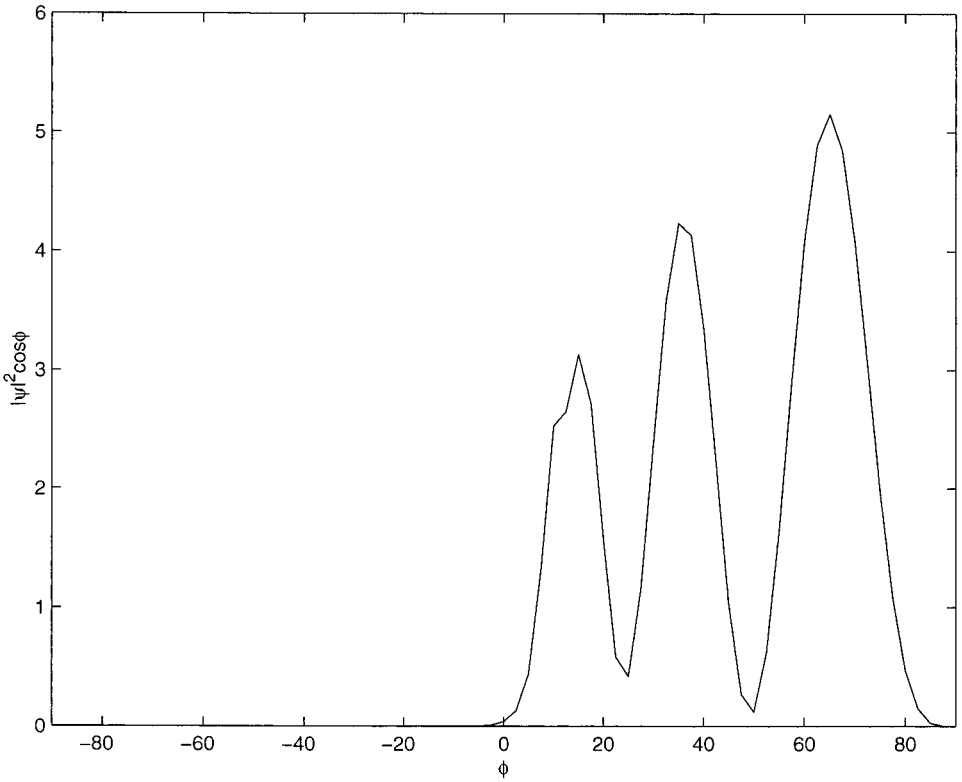

FIG. 7. Normalized $|\psi|^2 \cos\phi$ for two-jet flow, with forcing at 10°N.

$\langle|\psi|^2 \cos\phi\rangle$ begin to concentrate near zero. This concentration is already strong for $\eta \sim 0.15$–0.20, although the PDF still displays the hint of an oscillatory character. As η increases further, the PDF piles up near zero with little remaining trace of oscillations, especially near the pole.

6. Interpretation

The observed localization of planetary waves results from at least two causes: backscattering of waves by fluctuations in the wind field, and the appearance in the flow of critical lines. Considering the first cause, wave attenuation could occur in regions where wind fluctuations create either an imaginary index of refraction or a highly fluctuating real index of refraction. It was noted by Pandolfo and Sutera (1991) that fluctuations in the background velocity can lead to regions in the flow where the refractive index associated with the wave equation (7) is imaginary. An imaginary index of refraction creates decaying, not oscillatory, solutions. Passing through one of these regions, the amplitude of a wave is attenuated. As the noise level increases, these regions occupy a larger fraction of latitudes, and consequently the planetary wave energy is increasingly trapped in the vicinity of the source. Pandolfo and Sutera (1991) also showed that wave backscattering due to spatial fluctuations in a positive index of refraction could localize wave energy near its source. The other mechanism that is presumably important for localization is the appearance of critical lines. In the problem at hand these are latitudes at which the zonal-mean zonal velocity vanishes. The extent to which critical lines are absorbing, reflecting, or overreflecting remains controversial (e.g., Branstator 1983; Killworth and McIntyre 1985; Brunet and Haynes 1996; Campbell and Maslowe 1998), but without question they inhibit the dispersion of Rossby waves. Figure 9 shows the fraction of realizations in which the zonally averaged zonal wind is zero or negative as a function of latitude and η. As η increases, the chance occurrence of a nonpositive $U(\phi)$ increases, and the range over which $U(\phi)$ is often negative moves equatorward from the poles. Then, it is possible that the concentration of the PDF of $|\psi|^2 \cos\phi$ around zero, starting near the poles and moving equatorward as η increases, merely reflects the equatorward movement of the latitudes at which the wave is likely to first encounter a critical line.

Each of the three mechanisms of wave trapping discussed above participate in creating the PDFs of Figs. 5, 6, and 8. However, the role of imaginary indices of refraction and critical lines is minimal. This can be determined by an examination of Figs. 5, 6, and 9. Figure 9 shows that, even for high noise levels, critical lines are commonplace only in polar regions. The corresponding figure for the index of refraction (not shown) reveals

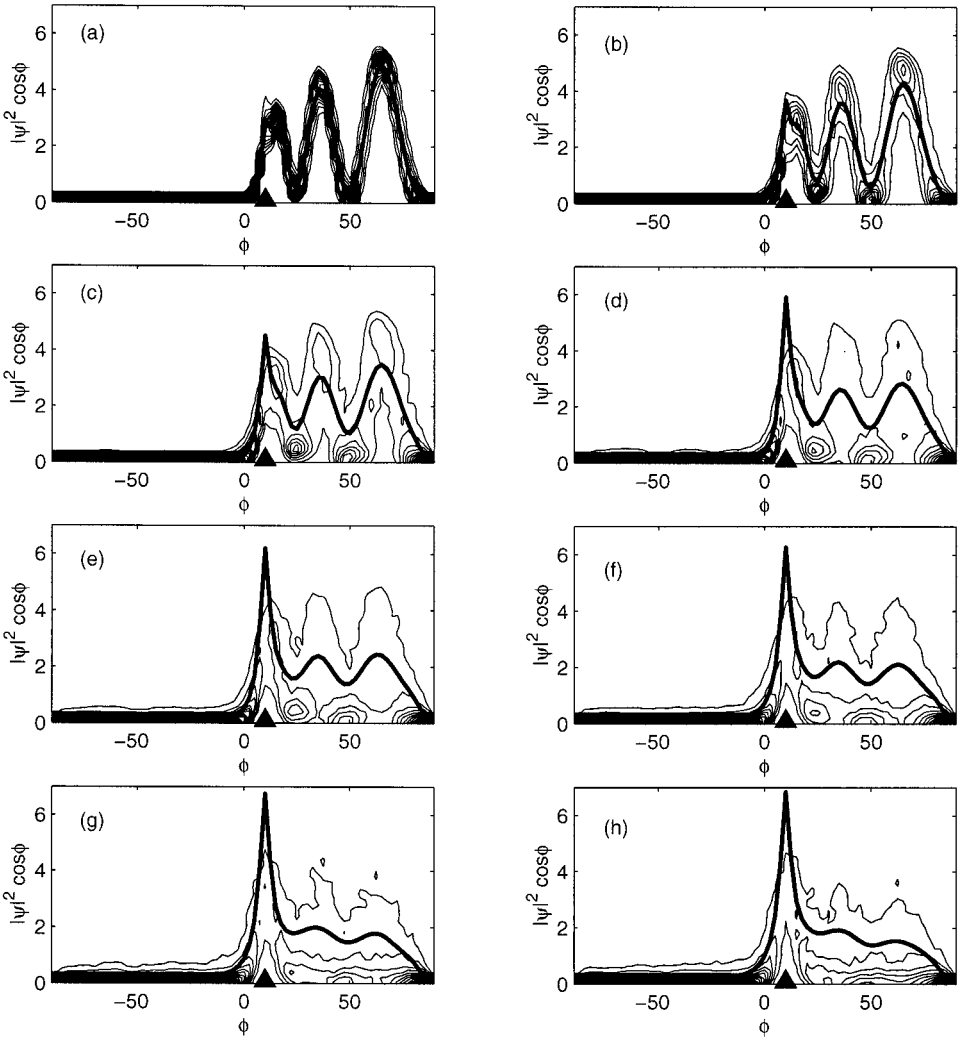

FIG. 8. Estimated PDF of $|\psi|^2 \cos\phi$ as a function of latitude for two-jet flow, for noise levels in increments of 0.05 from (a) $\eta = 0.05$ to (h) $\eta = 0.4$. The bold line is the sample mean $\langle|\psi|^2 \cos\phi\rangle$. The source location, $\phi_F = 10°$N, is marked by a black triangle. Contour interval: 0.025.

a similar distribution of imaginary realizations. This is because the wave restoring force is dominated by the advection of planetary vorticity by the perturbation field, so the index of refraction is imaginary only where the background wind is easterly (Pandolfo and Sutera 1991). In addition, the symmetry of wind fluctuations with respect to the equator present in Fig. 9 would be mirrored by the PDFs of Figs. 5 and 6 if critical lines (or imaginary indices of refraction) were important factors in determining the shape of PDFs. This symmetry would exist independently of the position of the forcing. Instead, the PDFs are symmetric with respect to the position of the source. Hence, it is unlikely that critical lines or negative indices of refraction are responsible for the localization observed in the PDFs displayed in Figs. 5 and 6. This indicates that it is the fluctuations of (mostly) real indices of refraction that are responsible for the wave backscattering that localizes wave energy around the source. Because of the similar localization behavior displayed in the Northern Hemisphere for the case of two-jet flow (Fig. 8), backscattering of wave energy by fluctuations is presumably responsible for localization in this case as well. The symmetry of the PDF with respect to the source and the monotonic decrease of wave amplitude away from the source in a positive index of refraction are the two characteristics of the occurrence of Anderson localization for waves dispersing in a random medium (Sheng 1995).

A mathematical analysis of the role of inhomogeneities in the wind field in generating wave backscattering leading to localization of wave energy is given in Imkeller et al. (2001). This study demonstrates that, in the limit of weak friction, the presence of fluctuations in U can introduce negative eigenvalues into the spectrum of the linear operator in (7), even in the absence of critical lines.

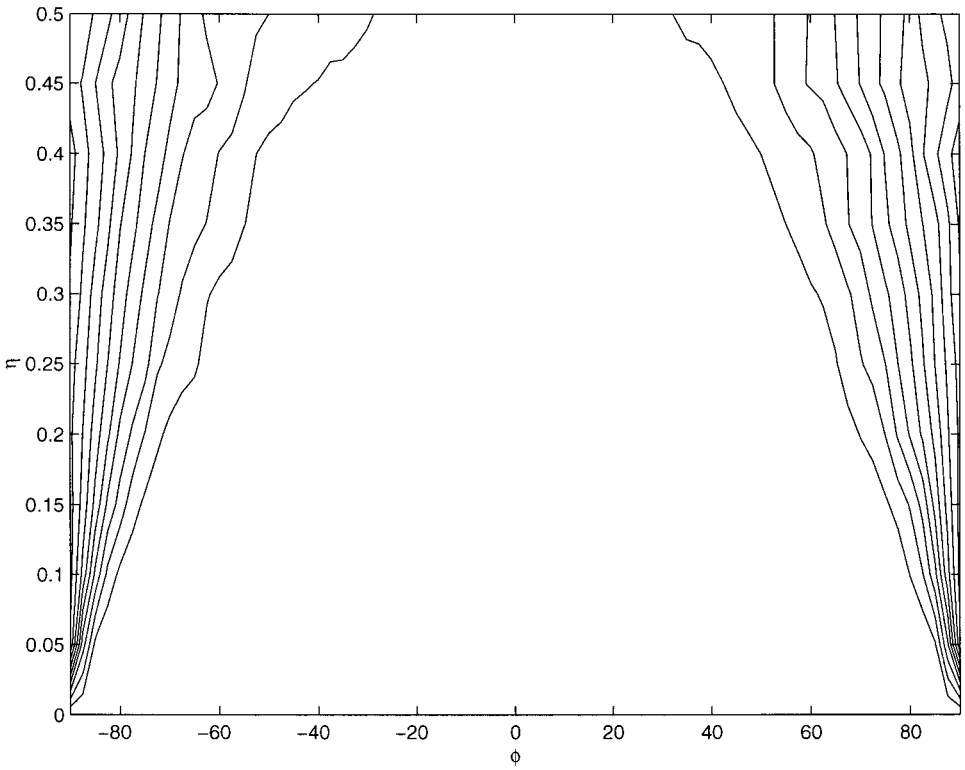

FIG. 9. Fraction of realizations in which $U(\phi) \leq 0$ as a function of ϕ and η. Contour interval: 0.05.

7. Conclusions

Using a Monte Carlo technique to sample realizations of a stochastic zonally averaged zonal velocity field, we have estimated the joint PDFs of the solution process to the nondivergent, barotropic vorticity equation linearized around these realizations. As was demonstrated in Pandolfo and Sutera (1991), fluctuations in the background flow $U(\phi)$ around a smooth mean $E\{U(\phi)\}$ can yield wave solutions with dispersion characteristics that are very different from those of waves propagating on $E\{U(\phi)\}$ itself. In particular, fluctuations can cause the wave energy to be trapped around the wave source. The extent of this trapping does not appear to be a simple linear function of the magnitude of the fluctuations. For low noise levels, the distribution of $|\psi|^2 \cos\phi$ merely broadens around the $\eta = 0$ value. As η increases, $\langle|\psi|^2 \cos\phi\rangle$ displays increasing poleward attenuation and the character of the PDF becomes less wavelike. As the noise level increases beyond $\eta \sim 0.15$, the PDF becomes increasingly concentrated near zero in the subpolar region, and in the midlatitudes as the noise increases even further (in response to a subtropical forcing).

The lowpass-filtered boreal winter data considered in section 2 indicate that the observed noise level is $\eta \sim$ 0.1–0.15 for zonal-mean zonal velocity at 500 mb. Hence, linearization around a smooth climatological flow can give only a rough qualitative description of wave dispersion since, as shown in Figs. 8b and 8c, $\langle|\psi|^2 \cos\phi\rangle$ differs substantially from its $\eta = 0$ character.

Branstator (1983) addressed the question of what velocity field would be an appropriate background flow around which to linearize the equations of motion. The results presented here indicate that linearization around a fluctuating background flow may produce results that are different than those obtained by linearizing around a smooth flow, and that physical intuition based on the latter may not be appropriate when dealing with realistic atmospheric flows.

The forcing used in this study is zonally invariant. To truly understand the dispersion of stationary wave energy in response to a forcing of finite zonal extent, we must work on the full sphere. In a future study, we will extend this analysis to a full spherical domain, and investigate the effects of fluctuations in the wind field (which may also vary zonally) on the response of the linearized equations of motion to zonally localized forcing.

Finally, the results of this study can be understood in at least two distinct ways. First, this analysis can be thought of as an investigation of the dispersion characteristics of stationary wavelike disturbances on a nonsmooth background flow. This interpretation implies a temporal separation of scales such that the adjustment time of the circulation to a stationary perturbation is much less than the timescale of changes in the back-

ground wind. As we have considered fluctuations in the 10-day lowpass-filtered winds, this separation of timescales holds only as a first-order approximation. A more accurate analysis would involve adding temporal variability to the problem.

Alternatively, this study may be regarded as an analysis of the *sensitivity* of the solutions to the linearized equations of motion to the background flow around which the linearization is carried out. Generally, smooth background flows are chosen for their simplicity, and not for their relevance to the actual circulation of the atmosphere. In fact, the long-term climatological average is a circulation whose neighborhood in phase space is rarely visited by the real atmosphere (Pandolfo 1993). In general, these background flows are forced to be solutions to the linearized equations of motion through the introduction of appropriate forcings, calculated a posteriori after the selection of the zonal-mean background state. This begs the question of the sensitivity of the character of the solutions to the basic state chosen, a question that this study addresses. The realizations of the background wind with fluctuations are then seen not so much as representing actual circulations in the atmosphere, but background states around which it is *equally plausible* to linearize as around the smooth flows. We find that the structure of the background wind can *qualitatively* affect the dispersion of energy from a localized source, for background flows that differ sufficiently from smooth flows.

These two interpretations of the results are distinct: the first is more physical, but involves an approximation concerning atmospheric relaxation and fluctuation timescales; the second is more a question of mathematics, but addresses a question that is of relevance to linearized theories of atmospheric dynamics. In a future study, we will relax the assumption of timescale separation, and consider the fully time-dependent propagation problem.

Acknowledgments. The authors would like to thank Cindy Greenwood, Phil Austin, Greg Lewis, Chris Jeffery, and Nicole Marshall for their helpful comments throughout the course of this project, and Peter Imkeller, Cécile Penland, and Prashant Sardeshmukh for helpful comments on an early draft of the manuscript. We also thank the three anonymous referees for comments that improved the paper. Adam Monahan was supported by the University of British Columbia and by the Crisis Points Group of the Peter Wall Institute for Advanced Studies, and Lionel Pandolfo was supported by a grant from the Natural Sciences and Engineering Research Council of Canada.

APPENDIX

Spectral Representation of R(ϕ)

Rather than generate $R(\phi)$ in direct space and then Fourier transform it, we chose to generate the noise process directly in spectral space. That is, we defined complex random variables $x_n, y_n \in \Re$ such that

$$R(\phi) = \sum_{m=-\infty}^{\infty} R_m e^{2im\phi}, \tag{A1}$$

where

$$R_m = x_m + iy_m. \tag{A2}$$

Because $R(\phi)$ is a real-valued process, we must have $R_{-m} = R_m^*$, that is,

$$x_m = x_{-m} \tag{A3}$$

$$y_m = -y_{-m}. \tag{A4}$$

We take x_m, y_m to be independent and identically distributed Gaussian random variables (RVs):

$$x_m, y_m \sim \mathcal{N}(0, \sigma_m), \tag{A5}$$

such that

$$E\{x_{m_1}x_{m_2}\} = \sigma_{m_1}^2 \delta_{m_1 m_2}, \tag{A6}$$

$$E\{x_{m_1}y_{m_2}\} = 0, \tag{A7}$$

$$E\{y_{m_1}y_{m_2}\} = \sigma_{m_1}^2 \delta_{m_1 m_2}. \tag{A8}$$

It follows that the joint PDF $p(x_m, y_m)$ satisfies

$$\begin{aligned} &p(x_m, y_m)dx_m dy_m \\ &\quad = p(x_m)p(y_m)dx_m dy_m \\ &\quad = \frac{1}{2\pi}\frac{1}{\sigma_m^2}\exp\left[-\frac{(x_m^2 + y_m^2)}{2\sigma_m^2}\right]dx_m dy_m \\ &\quad = \left(\frac{1}{2\pi}d\theta_m\right)\left[\frac{1}{\sigma_m^2}\exp\left(-\frac{|R_m|^2}{2\sigma_m^2}\right)|R_m|d|R_m|\right] \\ &\quad = [p(\theta_m)d\theta_m][p(|R_m|)d|R_m|], \end{aligned} \tag{A9}$$

where we have introduced the polar coordinates

$$R_m = |R_m| \exp i\theta_m. \tag{A10}$$

The joint distribution for x_m, y_m can then be written as a joint distribution for the independent RVs $|R_m|$ and θ_m, where the distribution of θ_m is uniform over $[-\pi/2, \pi/2]$.

The distributions of x_n, y_n must be specified so that (18)–(20) are satisfied. We have

$$\begin{aligned} &E\{R(\phi)R(\phi + \Phi)\} \\ &\quad = E\left\{\left(\sum_{m_1=-\infty}^{\infty} R_{m_1}^* e^{-2im_1\phi}\right)\left(\sum_{m_2=-\infty}^{\infty} R_{m_2} e^{2im_2(\phi+\Phi)}\right)\right\} \\ &\quad = \sum_{m_1=-\infty}^{\infty}\sum_{m_2=-\infty}^{\infty} E\{R_{m_1}^* R_{m_2}\}e^{2i(m_2-m_1)\phi}e^{2im_2\Phi}. \end{aligned} \tag{A11}$$

From equations (A6)–(A8),

$$E\{R^*_{m_1}R_{m_2}\} = E\{(x_{m_1} - iy_{m_1})(x_{m_2} + iy_{m_2})\} = 2\sigma^2_{m_1}\delta_{m_1m_2} \quad \text{(A12)}$$

so

$$E\{R(\phi)R(\phi + \Phi)\} = 2\sum_{m=-\infty}^{\infty} \sigma^2_m e^{2im\Phi}. \quad \text{(A13)}$$

Now, for the autocovariance function (20)

$$E\{R(\phi)R(\phi + \phi_0)\} = \sum_{n=-\infty}^{\infty} \rho_n e^{2in\Phi}, \quad \text{(A14)}$$

with

$$\rho_n = \sqrt{\frac{2\tau}{\pi}}\cosh(4\alpha\tau^2 n)\exp[-2(\alpha^2 + n^2)\tau^2]. \quad \text{(A15)}$$

Then we have that

$$\sigma^2_n = \frac{\rho_n}{2}. \quad \text{(A16)}$$

It was found in the experiments that the sample autocorrelation function of the synthetic data was a better match to that of the observations if ρ_0 was set to zero, in which case R_0 becomes a deterministic constant:

$$R_0 = 0. \quad \text{(A17)}$$

REFERENCES

Anderson, P. W., 1958: On the absence of diffusion in certain random lattices. *Phys. Rev. E,* **109,** 1492–1503.

Branstator, G., 1983: Horizontal energy propagation in a barotropic atmosphere with meridional and zonal structure. *J. Atmos. Sci.,* **40,** 1689–1708.

Brunet, G., and P. H. Haynes, 1996: Low-latitude reflection of Rossby wave trains. *J. Atmos. Sci.,* **53,** 482–496.

Campbell, L. J., and S. A. Maslowe, 1998: Forced Rossby wave packets in barotropic shear flows with critical layers. *Dyn. Atmos. Oceans,* **28,** 9–37.

Devillard, P., F. Dunlop, and B. Souillard, 1988: Localization of gravity waves on a channel with a random bottom. *J. Fluid Mech.,* **186,** 521–538.

Held, I. M., 1983: Stationary and quasi-stationary eddies in the extratropical atmosphere: Theory. *Large Scale Dynamical Processes in the Atmosphere,* B. J. Hoskins and R. P. Pearce, Eds., Academic Press, 127–168.

——, S. W. Lyons, and S. Nigam, 1989: Transients and the extratropical response to El Niño. *J. Atmos. Sci.,* **46,** 163–174.

Hoskins, B. J., and D. J. Karoly, 1981: The steady linear response of a spherical atmosphere to thermal and orographic forcing. *J. Atmos. Sci.,* **38,** 1179–1196.

——, and T. Ambrizzi, 1993: Rossby wave propagation on a realistic longitudinally varying flow. *J. Atmos. Sci.,* **50,** 1661–1671.

Imkeller, P., A. H. Monahan, and L. Pandolfo, 2001: Some mathematical results concerning the localisation of planetary waves in a stochastic background flow. *Proc. Workshop on Stochastic Climate Models,* Chorin, Germany, Birkhauser, in press.

Kalnay, E., and Coauthors, 1996: The NCEP/NCAR 40-Year Reanalysis Project. *Bull. Amer. Meteor. Soc.,* **77,** 437–471.

Karoly, D. J., 1983: Rossby wave propagation in a barotropic atmosphere. *Dyn. Atmos. Oceans,* **7,** 111–125.

Keller, J. B., and G. Veronis, 1969: Rossby waves in the presence of random currents. *J. Geophys. Res.,* **74,** 1941–1951.

Kiladis, G. N., and K. M. Weickmann, 1992a: Circulation anomalies associated with tropical convection during northern winter. *Mon. Wea. Rev.,* **120,** 1900–1923.

——, and ——, 1992b: Extratropical forcing of tropical Pacific convection during northern winter. *Mon. Wea. Rev.,* **120,** 1924–1938.

——, and ——, 1997: Horizontal structure and seasonality of large-scale circulations associated with submonthly tropical convection. *Mon. Wea. Rev.,* **125,** 1997–2013.

——, G. A. Meehl, and K. M. Weickmann, 1994: Large-scale circulation associated with westerly wind bursts and deep convection over the western equatorial Pacific. *J. Geophys. Res.,* **99,** 18 527–18 544.

Killworth, P. D., and M. E. McIntyre, 1985: Do Rossby-wave critical layers absorb, reflect, or over-reflect? *J. Fluid Mech.,* **161,** 449–492.

Kotani, S., 1986: Lyapunov exponents and spectra for one dimensional Schroedinger operators. *Contemp. Math.,* **50,** 277–286.

Lau, N.-C., 1997: Interactions between global SST anomalies and the midlatitude atmospheric circulation. *Bull. Amer. Meteor. Soc.,* **78,** 21–33.

Li, L., and T. R. Nathan, 1994: The global atmospheric response to low-frequency tropical forcing: Zonally averaged basic states. *J. Atmos. Sci.,* **51,** 3412–3426.

——, and ——, 1997: Effects of low-frequency tropical forcing on intraseasonal tropical–extratropical interactions. *J. Atmos. Sci.,* **54,** 332–346.

Pandolfo, L., 1993: Observational aspects of the low-frequency intraseasonal variability of the atmosphere in middle latitudes. *Advances in Geophysics,* Vol. 34, Academic Press, 93–174.

——, and A. Sutera, 1991: Rossby waves in a fluctuating zonal mean flow. *Tellus,* **43A,** 257–265.

Pedlosky, J., 1987: *Geophysical Fluid Dynamics.* Springer-Verlag, 710 pp.

Robinson, W. A., 1996: Does eddy feedback sustain variability in the zonal index? *J. Atmos. Sci.,* **53,** 3556–3569.

Sengupta, D., 1994: Localization of Rossby waves over random topography: Two-layer ocean. *J. Phys. Oceanogr.,* **24,** 1065–1069.

——, L. I. Piterbarg, and G. M. Reznik, 1992: Localization of topographic Rossby waves over random relief. *Dyn. Atmos. Oceans,* **17,** 1–21.

Sheng, P., 1995: *Introduction to Wave Scattering, Localisation, and Mesoscopic Phenomena.* Academic Press, 339 pp.

Thomson, R. E., 1975: The propagation of planetary waves over a random topography. *J. Fluid Mech.,* **70,** 267–285.

Trenberth, K. E., G. W. Branstator, D. Karoly, A. Kumar, N.-C. Lau, and C. Ropelewski, 1998: Progress during TOGA in understanding and modelling global teleconnections associated with tropical sea surface temperatures. *J. Geophys. Res.,* **103,** 14 291–14 324.

Vanneste, J., 2000a: Enhanced dissipation for quasi-geostrophic motion over small-scale topography. *J. Fluid Mech.,* **407,** 105–122.

——, 2000b: Rossby-wave frequency change induced by small-scale topography. *J. Phys. Oceanogr.,* **30,** 1820–1826.

Yang, G.-Y., and B. J. Hoskins, 1996: Propagation of Rossby waves of nonzero frequency. *J. Atmos. Sci.,* **53,** 2365–2378.